CHROM. 24 818

Dispersion in packed-column hydrodynamic chromatography

Gerrit Stegeman, **Johan** C. Kraak and Hans **Poppe***

Laboratory for Analytical Chemistry, University of Amsterdam, Nieuwe Achtergracht 166, 1018 WV Amsterdam (Netherlands)

ABSTRACT

Zone broadening of dissolved polystyrenes in packed-column hydrodynamic chromatography (HDC) was studied for a column filled with 1.5-μm monodisperse non-porous particles. The reduced plate heights were observed to be almost constant with mobile phase velocity for reduced mobile phase velocities in a range 2–>150. In this velocity range, reduced plate heights well below 2 were obtained for polymer samples with molecular masses of 2200, 43 900 and 775 000. A comparison was made between measured plate heights and chromatographic theories of zone spreading. The effects of polymer size, polydispersity and polymer hydrodynamics on the measured plate heights are discussed.

INTRODUCTION

In hydrodynamic chromatography (HDC), macromolecules and particles are separated according to size. The separation mechanism takes advantage of the non-uniform flow profile in an open tube or in the interstitial space in packed columns [1–6]. Because of their size, large molecules are confined more than smaller molecules in the centre of a flow channel. As the streamline velocity is higher in the central part of the channel, large molecules are eluted before smaller molecules.

Research in HDC has so far mainly been aimed at describing the migration behaviour of macromolecules, in both theoretical and experimental studies [2–6], and relatively little attention has been paid to dispersion.

In this paper, we focus on the dispersion of random coil polymers in packed columns. In contrast to common chromatographic practice,

the size of the solutes is no longer infinitely small compared with the inter-particle flow channels. This means that wall exclusion and hydrodynamic particle-wall interactions may come into play.

Brenner and Gaydos [3] showed that a theoretical analysis of the dispersion of **finite**-sized solutes in open capillary tubes is severely complicated compared with infinitely small solutes. Modifying the Taylor-Aris dispersion theory to account properly for the finite solute to tube radius ratio appeared to be an elaborate process, even for apparently simple solutes such as isolated, neutrally buoyant, rigid spheres. For less symmetrical flow channels or for other than spherical homogeneous particles, realistic **model**ling becomes extremely involved.

In packed columns, rigorous calculations of the dispersion of finite-sized solutes are impossible because of the complex geometry of the interstitial flow channels. In several studies, therefore, attempts have been made to apply the dispersion models for open capillaries to packed columns. This is done by representing the **inter**-

---

* Corresponding author.

stitial flow channels as cylindrical tubes. In the simplest approach, a packed column is seen as a bundle of distinct capillaries without interconnections. This model evidently is an oversimplification as it does not describe the random mixing processes that occur in packed beds. Indeed, the predicted dispersion behaviour was found to be not in very good agreement with experimental observations [7]. Mixing effects are better accounted for when the interstitial channels are depicted as a capillary network, such as proposed by Saffman [8]. Silebi and Viola [9] modified Saffman's analysis by including wall exclusion resulting from the finite solute size. The dispersion behaviour as predicted by this modified model was in fairly good agreement with experimental results, although the effect of solute size on dispersion was not described successfully. A more sophisticated theory of the dispersion of finite-sized solutes in porous media was developed by Brenner and Adler [10,11]. However, from their general theory, it is not yet possible to derive simple relationships between dispersion in packed chromatographic columns and experimentally accessible quantities, because of the complex structure of the local interstitial velocity field.

We follow a different strategy, by starting with accepted chromatographic dispersion theories for zero-sized solutes in packed columns. Such theories have been developed by Giddings [12], Horváth and Lin [13], Huber [14] and Done and Knox [15]. Their models, which have been tested by a wealth of experimental data, are now well established. The most comprehensive analysis of dispersion in the (inter-particle) mobile phase was carried out by Giddings [16,17]. He provided a detailed description of the various contributions to zone spreading and estimated their magnitude. Part of this theory, which is most relevant to our work, will be briefly outlined below.

THEORY

Giddings' general equation for the dispersion in the mobile phase in terms of the plate height H is

$$H = H_L + \sum_i \left(\frac{1}{\frac{1}{H_{D,i}} + \frac{1}{H_{f,i}}} \right) \tag{1}$$

where the H terms are the different plate height contributions which will be treated subsequently. H_L is the plate height contribution from longitudinal molecular diffusion. This term describes the zone spreading along the column axis due to random thermal motion. In packed columns H_L can be written as

$$H_L = 2\gamma D_m / v \tag{2}$$

where γ is an obstructive factor accounting for the obstructions to diffusion along a straight line imposed by the packing particles and is cu. 0.6 for randomly packed impervious spheres [16,18], D_m is the diffusion coefficient in the mobile phase and v is the average mobile phase velocity. H_L is predicted by eqn. 2 to be larger for small molecules with large D_m values than for macromolecules with lower D_m values.

The second term (in parentheses) in eqn. 1, called the coupling terms, arises from the non-uniformities of flow velocity in the mobile phase. The summation sign allows for the inclusion of different types of velocity non-uniformities (denoted by i). The exchange of molecules between different velocity domains can occur due to flow and diffusion. Each parameter $H_{D,i}$ describes the plate height corresponding to a non-uniformity i when the flow dispersion would be counteracted by diffusion exclusively. When, in contrast, the exchange between velocity regimes is solely effected by random flow, dispersion resulting from velocity inequalities is represented by a parameter $H_{f,i}$. Coupling of $H_{D,i}$ and $H_{f,i}$, as given in each term of the summation in eqn. 1, amounts to the addition of lateral fluxes due to diffusion and convection in the exchange of molecules between flow paths of unequal velocities.

According to Giddings, the expression for $H_{D,i}$ is

$$H_{D,i} = \omega_i d_p^2 v / D_m \tag{3}$$

where ω_i is a constant for a given velocity inequality i and d_p is the diameter of the packing

particles. $H_{f,i}$ (often called the eddy diffusion term) can be written as

$$H_{f,i} = 2\lambda_i d_p \tag{4}$$

where λ_i is another constant, which depends on the type of velocity inequality.

For columns with non-porous packing particles, four sources of velocity non-uniformities are distinguished: (1) Trans-channel: the velocity in the centre of narrow inter-particle flow channels is higher than near the walls. This is analogous to the convective dispersion in open-tube flow after Taylor-Aris. (2) Short-range inter-channel: in some channels, the velocity is higher than in channels nearby because of differences in shape, openness and obstructions. (3) Long-range inter-channel: in some regions, the velocity is higher than in others because of differences in void geometry. This effect resembles (2) but is of longer range. (4) Trans-column: the velocity is potentially higher near the column wall than at the column centre, owing to looser packing near the wall. Approximate values for the constants ω_i and λ_i as given by Giddings [16] are summarized in Table I.

For a more universal representation of dispersion it is convenient to use dimensionless quantities. In terms of the dimensionless reduced plate height $h = H/d_p$ and reduced velocity $\nu = v d_p/D_m$, the equation for the mobile phase plate height becomes

$$h_{kin} = \frac{2\gamma}{\nu} + \sum_i \left(\frac{1}{\dfrac{1}{\omega_i \nu} + \dfrac{1}{2\lambda_i}} \right) \tag{5}$$

where h_{kin} is used to indicate that only kinetic

TABLE I

APPROXIMATE MAGNITUDES OF THE PARAMETERS ω_i AND λ_i

Type of velocity non-uniformity	ω_i	λ_i
(1) Trans-channel	0.01	0.5
(2) Short-range inter-channel	0.5	0.5
(3) Long-range inter-channel	2	0.1
(4) Trans-column	$0.001\rho^{2\,a}$	$0.02\rho^{2\,a}$

$^a \rho$ = Column-to-particle diameter ratio.

contributions to zone broadening are considered. Other, non-kinetic, contributions will be treated in the discussion of the experimental results.

Although it is generally recognized that eqn. 5 has a sound theoretical basis, it does not reproduce experimental data well when the proposed values for λ_i and ω_i are used [19]. This can be ascribed largely to a failure to account correctly for trans-column effects. Giddings predicted an ever-increasing trans-column plate height with increasing column to particle diameter ratio ρ. Since then, it has been found experimentally that ρ does not affect plate heights to the extent of Giddings' predictions. Knox and Parcher [20] found that the trans-column plate height increases with ρ until $\rho \approx 10$ and then attains a constant value. In later work, it was even argued that trans-column effects are likely to become negligible for very large values of ρ [21].

Based on our results for a 4.6 mm I.D. column filled with 1.5-μm particles, Giddings' original theory predicts a trans-column plate height of at least 10^4 for reduced velocities exceeding 1. This is indeed far from our measured values, which were below 2, as will be shown later.

In Fig. 1, the mobile phase plate height contributions according to Giddings are shown for a column with non-porous particles. The
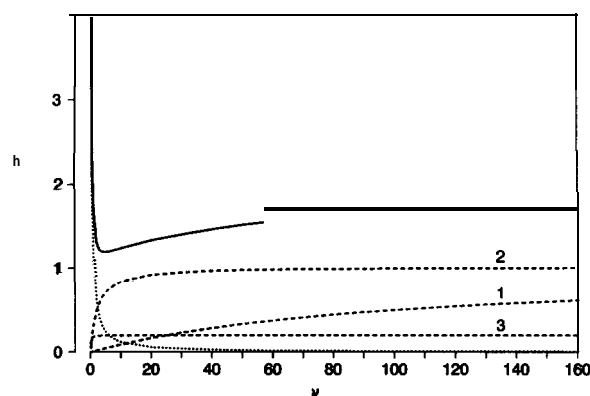

Fig. 1. Mobile phase plate height for unsorbed solutes in an infinite diameter column with non-porous particles. Plate height contributions according to Giddings (eqn. 5). Dotted line, longitudinal molecular diffusion; dashed lines, coupling terms with (1) trans-channel, (2) short-range inter-channel and (3) long-range inter-channel contributions; solid line, sum curve. ω_i and λ_i are taken from Table 1; $\gamma = 0.6$.

trans-column effect is not included. As **Giddings'** **trans-column** effect results from the influence of the wall on the packing density, Fig. 1 represents the plate height contributions for a so-called "infinite diameter column" (Le., a column in which the solutes **cannot** reach the region of disturbed packing near the wall). The reduced velocity range in Fig. 1 corresponds to the range that will be covered by our measurements. It is obvious that at low reduced velocities, the plate height is dominated by the longitudinal molecular diision term. After the summed curve has passed through a minimum at $\nu = 5$, h_{kin} is determined mainly by the coupling terms. Note that the relative importance of each of the coupling terms can vary strongly with velocity.

Starting from Giddings' theory, Kennedy and Knox [22] derived a simpler, semi-empirical relationship for h, which in general fits experimental data well. In the Knox equation, the coupling process is approximated by a power term $\alpha\nu^n$ leading to [22]

$$h_{kin} = \frac{2\gamma}{\nu} + \alpha\nu^n \qquad (6)$$

where α is a measure of the quality of the packing; α is usually within the range OS-l.5 for a well packed column [23], having a typical value of 1 [17,24]. Values of α below 0.5 have frequently been found for columns with $\rho < 10$ [20,25,26], but not often for $\rho > 10$ [22,27]. The exponent n is usually found to be cu. 0.33. When wall effects are eliminated n has been found to be much smaller. For these infinite diameter columns n values as low as 0.20 have been found by Knox and co-workers [20,27] using non-porous glass beads as packing particles. Hence the particular shape of the Knox equation appears to reflect the influence of wall effects.

In Fig. 2, two forms of the Knox equation are shown representing plate height contributions for unsorbed solutes in (1) an infinite diameter column and (2) a walled column with non-porous particles. The factors α and n were determined by Knox and co-workers from **experimental** data for non-porous glass beads [22,27]. The most important difference between the infinite diameter column and the walled column is evidently
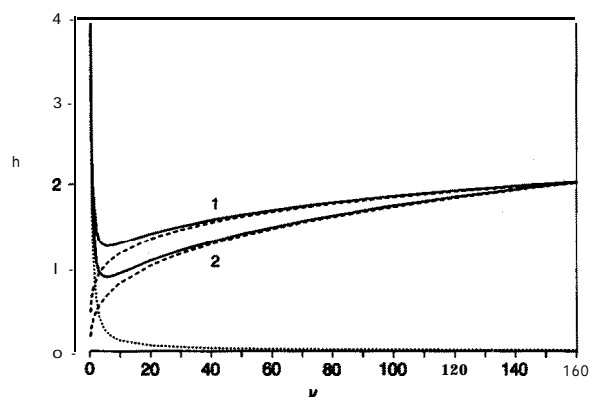

Fig. 2. Two forms of the Knox equation for the mobile phase plate height of unsorbed solutes in (1) an infinite diameter column and (2) a walled column with non-porous particles (eqn. 6). Dotted tine, longitudinal molecular diffusion; dashed lines, contribution from the complex flow pattern, $\alpha\nu^n$, for (1) an infinite diameter column with $\alpha = 0.73$ and $n = 0.20$ [27] and (2) a walled column with a $= 0.37$ and $n = 0.33$ [20,22]; solid line, sum curve. In both instances $\gamma = 0.6$.

the different slope of the summed curves at higher reduced velocities. For the infinite diameter column, h *rises* more gradually with ν than for the walled column.

Both the Knox semi-empirical equations, which were derived using a curve-fitting procedure, and Giddings' theory, which is more directly related to the transport phenomena in a packed column, will be used in this study of dispersion in packed-column HDC.

EXPERIMENTAL

Materials and chemicals

The HDC column used was a 150 *x 4.4 mm* I.D. stainless-steel column (Chrompack, **Middelburg**, Netherlands), which was laboratory packed with monodisperse non-porous silica spheres. The packing particles were a kind gift from Professor K.K. Unger (Johannes Gutenberg Universitat, Mainz, Germany). The size and the size distribution of the particles were determined from electron micrographs. Measurement of the diameter of 50 particles revealed an average particle diameter of 1.50 μm. The relative standard deviation for the diameter of a single bead was 2.3%. More detailed information about the
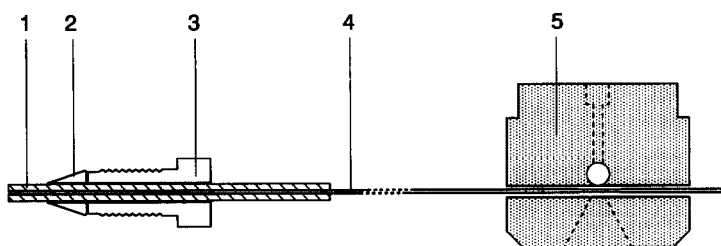
Fig. 3. Detection capillary with column connection. 1 = PTFE tube, 1.59 mm (1/16 in.) O.D. and 330 μm I.D.; 2 = laboratory-made PTFE ferrule; 3 = stainless-steel nut; 4 = fused-silica capillary, 300 pm O.D. and 100 μm I.D.; 5 = capillary flow cell holder with focusing lens.

packing particles, the packing procedure and the column characteristics are presented elsewhere [28].

The solvent used was analytical-reagent grade tetrahydrofuran (THF) from Merck (Darmstadt, Germany). Before use, THF was filtered through a 0.1-μm inorganic membrane filter (Anodisc 47; Anotec, **Banbury**, UK).

The solutes used were analytical-reagent grade toluene (Merck) and polystyrenes (PS) having a relative weight-average molecular mass (M_w) of 2200 (Merck), 43900 (Toyo Soda, Tokyo, Japan) and 775 000 (**Toyo** Soda). The **polydis**-persity P of the polymers was less than 1.06, 1.01 and 1.01, respectively, according to the manufacturer. The polymer concentrations used were 0.08 mg/ml.

Apparatus

The experimental set-up was built up from conventional HPLC equipment. A Spectroflow 400 HPLC pump (ABI, Ramsey, NJ, USA) was used for solvent delivery. A pneumatically driven injection valve with a Model **Ci4Wi**1-μl internal sample loop (VICI, Houston, TX, USA) was modified for high-speed switching by means of a speed-up kit (VICI). The detector was a Spectroflow 757 variable-wavelength UV detector (ABI), operated at 210 nm. The conventional UV detection cell was replaced with a capillary flow cell holder (ABI) in order to decrease external peak broadening. A small length of a 15 cm × 100 μm I.D. fused-silica capillary, which was directly coupled to the column outlet, served as a detection cell with a volume of less than 10 nl. This part of the set-up is outlined in Fig. 3. Retention times were measured using a Model

3390A integrator (Hewlett-Packard, Avondale, PA, USA). Plate heights were determined from the peak widths at half-height, using recorder drawings from a Kompensograph 3 strip-chart recorder (Siemens, Karlsruhe, Germany).

RESULTS AND DISCUSSION

In Fig. 4, the measured plate heights are plotted against v for all test solutes used. It appears that the plate heights, measured for PS 43 900 and PS 775 000, are almost independent of mobile phase velocity and increase only slightly with increase in velocity. Moreover, for both polymers the plate heights found are almost the same. The smaller solutes toluene and PS 2200 showed a stronger velocity dependence of H. For these solutes the increase in H with decreasing velocity is evidently caused by the longitudinal molecular diffusion terms H_L.
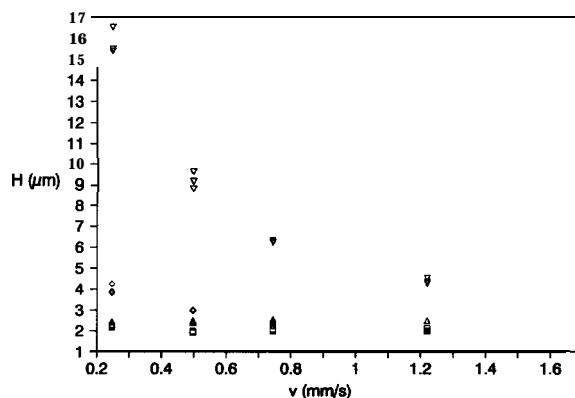
The very low plate heights found for the

Fig. 4. Plate height versus mobile phase velocity for solutes in THF. V = **Toluene**; 0 = PS 2200; □ = PS 43 900; A = **PS 775 ooo**.

higher molecular masses **are** of great importance for high-resolution separations in HDC. In addition, as *H* is almost independent of velocity, high-speed separations are possible without loss of resolution. These aspects are treated more extensively elsewhere [28].

Calculating plate heights from the peak width at half-height is only allowed when the peaks are sufficiently symmetrical. The peak shapes for the solutes used were observed to be symmetrical except for a slight tailing effect. **Asymmetry** factors, measured at one tenth of the peak height, were 1.1 (for toluene) to 1.3 at the lowest eluent velocity. Peak tailing was observed to increase with eluent velocity. At the highest velocity, asymmetry factors up to 1.6 were measured. The peak asymmetry for the polymers peaks was found to depend strongly on polymer concentration. At higher concentrations than those used for Fig. 3, peak **asymmetry** increased. **This** effect was more pronounced for higher molecular masses. Also, replacing the **100-**μm I.D. tubing between the injector and column by **250-**μm I.D. tubing worsened the peak shapes and increased the peak widths, especially for the higher molecular masses. The latter observation indicates that extra-column effects may be partly responsible for observed peak **asymmetry**.

The experimental results from Fig. 4 are plotted in reduced form in Fig. 5, together with the sum curves from Figs. 1 and 2. As predicted by chromatographic theory, the measured reduced plate heights all fall on a single curve. Comparing the experimental results with the theoretical lines, it is striking that they do not agree well with Knox's empirical line for a walled column. At velocities beyond the minimum in the plate height curve, the measured plate heights appear to depend much less on ν than predicted. The match cannot be improved if we choose a different value for α. Clearly, the exponent *n* in the Knox equation is too high to fit our results. Both lines for the infinite diameter column, which deviate from one another only slightly, correspond much better to experiment. The exponent *n* = 0.20 in the Knox equation is still too high to match the measured data, but the agreement is much better than for *n* = 0.33. In terms of the slope of the curve at higher
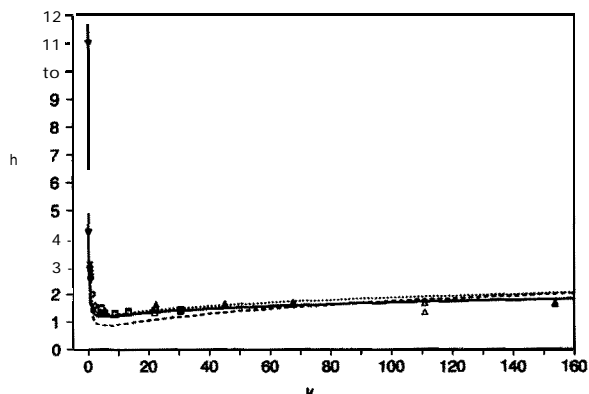

Fig. 5. Reduced plate height versus reduced velocity. Measured data: ∇ = toluene (D_m = 2.66 × 10^{-9} m^2/s [29]); 0 = PS 2200 (D_m = 4.49 × 10^{-10} m^2/s [30]); $\square$ = PS 43 900 (D_m = 8.31 × 10^{-11} m^2/s [30]); A = PS 775 000 (D_m = 1.65 × 10^{-11} m^2/s [30]). The theoretical lines are the sum curves from Figs. 1 and 2. Solid line, Giddings, infinite diameter column; dotted line, Knox, infinite diameter column; dashed line, Knox, walled column.

velocities, the theoretical line by Giddings corresponds best to our experimental results.

Fig. 5 seems to indicate that a trans-column effect is absent or at least negligible in our measurements. This can be made more convincing when we look in more **detail** at the **trans**-column velocity **inequalities**.

The effect of the different packing structure near the column wall on axial dispersion was investigated by Knox *et al.* [27]. They concluded that the wall region of disturbed packing extends about 30 particle diameters inwards from the wall, much deeper than suggested in earlier work [20]. The extent to which this wall region affects axial dispersion depends on the fraction of the column cross-sectional area, occupied by the **annulus** of irregular packing. The effect of the wall region on dispersion thus depends strongly on p. For very large values of ρ (>1000), the effect of the wall region is likely to become negligible [21], in contrast to Giddings' prediction of an ever increasing plate height with increasing ρ.

In our column, ρ is as high as 3067, owing to the very small particles used. Assuming a disturbed wall region of 30 particle diameters, this layer still only covers 4% of the cross-sectional area of our column. This fraction is so small that

its effect on the peak shape is probably negligible. Even if wall effects do slightly change the peak shapes, they will not in the first place affect the peak width at half-height (which was used for our plate height calculations), but rather broaden the base of the peaks.

Disturbance of the packing near the wall is not the only source of trans-column velocity variations. Knox et al. [27] also measured small velocity variations in the central part of the column. They observed a slight increase in velocity with increasing distance from the column axis. The packing inhomogeneity causing this type of trans-column effect is believed to depend strongly on the packing method and on the uniformity of the packing particles [16,27]. As a major source, it has been put forward that during packing, larger particles tend to settle near the column wall and smaller particles near the centre. The use of very monodisperse packing particles may help to minimize trans-column velocity variations. Our particles being more uniform than those used by Knox and co-workers may be the reason why the slope of our h-v curve is smaller than their curve for infinite diameter columns [20,27].

A negligible trans-column contribution may be the reason why our measured data closely resemble both the theoretical and the empirical lines for an infinite diameter column rather than the empirical line for a walled column. It is, however, too early to conclude that dispersion in HDC is now clarified. Complications, e.g., those arising from the finite solute size, and effects of polydispersity on measured plate heights, have not been considered so far. These aspects are discussed below.

Polydispersity

In the molecular mass distribution of the polymers used is not sufficiently narrow, **polydispersity** will increase the peak width and lead to higher apparent plate heights. Knox and **McLennan** [31] studied the effect of polydispersity on the measured plate height in size-exclusion chromatography (SEC). They obtained the following equations for the combined dispersion due to kinetic processes and polydispersity in SEC:

$$h_{app} = h_{kin} + h_{poly} \tag{7}$$

where

$$h_{poly} = \left(\frac{L}{d_p}\right)(P-1)(1+\beta)\left(\frac{S}{V_R}\right)^2 \tag{8}$$

h_{app} is the apparent (or measured) reduced plate height and h_{kin} and h_{poly} are the kinetic and polydispersity contributions. In the **polydispersity** term, L is the column length, β is a weak function of $(P-1)$ and has a value of about 1, S is the negative inverse slope of the calibration curve of $-d(V_R)/d(\ln M)$ and V_R is the elution volume of a solute.

It was shown that even in moderately efficient SEC columns, polydispersity is the dominating term in h_{app} unless P is well below 1.01. Whether polydispersity has an equal impact in HDC is easily investigated, as eqns. 7 and 8 are also valid in HDC. For a rough comparison of the effect of polydispersity on h_{app} in SEC and HDC, a comparison of the most relevant parameters h_{kin} and S suffices. In HDC, h_{kin} is usually much smaller than in SEC because of the absence of slow mass transfer between the pore space and the inter-particle channels [32]. In HDC the parameter S, describing the molecular mass selectivity, is not constant with molecular mass, because of the non-linear calibration graph. At the flattest part of the calibration graph the molecular mass selectivity may be as high as in conventional SEC. From this it appears that the impact of polydispersity on plate height in HDC may even be larger than in SEC.

Using eqns. 7 and 8, a more accurate estimate of the effect of polydispersity on the measured plate height can be made. In order to calculate h_{poly} for the polymer fractions used, the values of $(S/V_R)^2$ were determined from the experimental calibration graph which is shown in ref. 28. The values found were 1.39 $x10^{-5}$ for PS 2200, 3.78 $X10^{-4}$ for PS 43 900 and 6.19 $X10^{-3}$ for PS 775 000. Note that the difference in $(S/V_R)^2$ values reflects the distinction in molecular mass selectivity for the polymer samples. Here the column selectivity is clearly highest for PS 775 000 as a result of the curvature of the calibration graph.

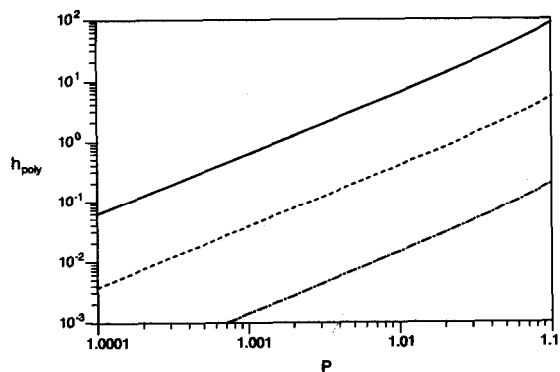Based on the $(S/V_R)^2$ values, the plate height

Fig. 6. Contribution from polydispersity to the reduced plate height for (dot-dashed line) PS 2200, (dashed line) PS 43 900 and (solid line) PS 775 000.

contribution from polydispersity, h_{poly}, is calculated as a function of polydispersity in Fig. 6.

For PS 2200, a polydispersity of 1.06 means that $h_{poly} = 0.1$. This is already relatively large compared with the measured reduced plate heights. For PS 43 900, h_{poly} is 0.4 for the specified polydispersity ceiling value of 1.01. Such a large value of h_{poly} should have increased the measured plate heights significantly compared with those for PS 2200. From Fig. 5 it appears, however, that the measured plate heights for PS 43 900 and PS 2200 are on a smooth curve and are not visibly shifted. Probably the actual polydispersity of the PS 43 900 sample is smaller than the maximum value specified by the manufacturer.

For PS 775 000, the manufacturer's value (P = 1.01) yields a calculated h_{poly} value of 6. This value is almost four times higher than the measured (total) reduced plate height. Here it is clear that the stated ceiling value is much higher than the actual polydispersity. The actual polydispersity of PS 775 000 cannot be determined exactly from our measurements as we do not know the precise magnitude of h_{kin}. If h_{app} were entirely determined by polydispersity (i.e., $h_{app} = h_{poly} = 1.5$), we calculate a polydispersity of 1.002. Even this low value is actually still too high as it implies that $h_{kin} = 0$. A more realistic estimate of h_{poly}, on the basis of the plate heights measured for the smaller polymers, indicates that h_{poly} does not exceed 0.3, or in other words $P < 1.0005$.

Large differences between actual polydisper-

sities and ceiling values have been reported before in thermal field flow fractionation [33,34]. The explanation for these differences is that the stated ceiling values are very conservative estimates. Given the error in the individual determinations of the weight- and number-average molecular masses and considering the scatter in these values obtained by various techniques, the specified polydispersities may well be much higher than the actual polydispersities [35].

From the preceding discussion, it appears that the polydispersity of the polymer samples is an important plate height contribution in the high selectivity region of the HDC calibration graph. The separation power of the column used is so high that even for true polydispersities as low as 1.01 the measured plate heights are expected to be dominated by polydispersity. Even though the true polydispersities of the polymer samples used may be much lower than 1.01, the measured plate heights (for PS 43 900 and PS 775 000) are still likely to include a significant polydispersity contribution. In order to be assured that the measured plate heights are equal to h_{kin}, polymer samples with an extremely narrow molecular mass distribution, preferably real monodisperse samples, are required. Unfortunately, such samples are not available in the range of higher molecular masses. Another way to isolate h_{kin} is to measure h_{app} at a fixed eluent velocity on columns of different lengths (see eqns. 7 and 8). Extrapolation of h_{app} to zero column length should give values of h_{kin}. This procedure was not employed by us. As a result, we do not know the absolute magnitude of h_{kin}. The dependence of h_{kin} on ν can nevertheless still be obtained from Fig. 5 as polydispersity shifts the $h_{kin}-\nu$ curve by a fixed amount (equal to h_{poly}) towards higher apparent plate heights.

Polymer size

When the size of the flow channels is not enormously large compared with the size of the solute molecules, several effects that are not included in dispersion theories for infinitely small molecules may become of importance.

Exclusion regions. Owing to the finite size of the molecules, the centre of mass of a solute molecule is excluded from flow regions in the flow channel, within a distance of one effective

polymer radius from the wall. For flow in narrow channels between parallel plates and for flow in open tubes, the effect of wall exclusion on dispersion (leaving out hydrodynamic wall effects) can readily be expressed in modifications of plate height models for zero-sized solutes [2,36]. DiMarzio and Guttman [2] developed an expression for the convective contribution to axial dispersion for solute particles or radius r_p in open tubes of radius r_c. They found that the finite solute size reduces the convective term by a factor of $[1-(r_p/r_c)]^6$ compared with the limit for infinitely small molecules. In capillary HDC, where r_p/r_c ratios are usually in the range 0.01–0.3, the reduction of plate heights can be profound.

In packed columns, the effect of wall exclusion on dispersion cannot be described as precisely as for open capillary tubes, so a more approximate approach is required. Exclusion layers are expected to have a predominant influence on the convective dispersion in a single flow channel by reducing the cross-sectional diffusion distance, as illustrated in Fig. 7. In Giddings' theory this implies a reduction of the trans-channel plate height term. As wall exclusion is a short-range effect, it will not in the first place influence the other coupling terms.

There is, however, one effect of longer range we might have to consider, namely the effect of exclusion on the average solute velocity. Wall exclusion causes the average velocity of finite sized solutes to be higher than the average
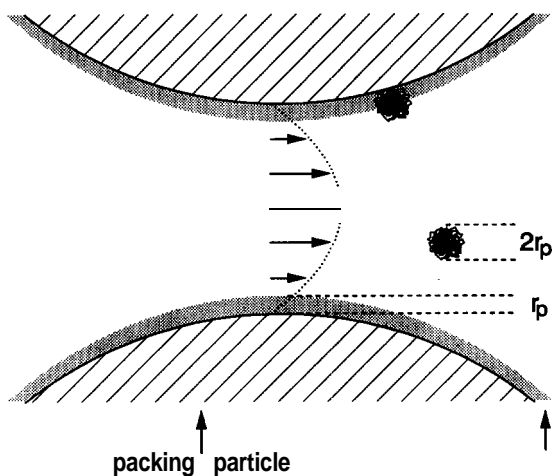

packing   particle

Fig. 7. Wall exclusion in packed columns.

solvent velocity. This exclusion effect is much stronger in narrow than in wider channels. Exclusion may thus partly compensate for the lower average eluent velocity in narrower flow channels and more densely packed column regions. It can therefore reduce the difference in solute velocity between channels of different cross-sectional size. In terms of Giddings' dispersion theory, this would reduce the inter-channel velocity variations for finite-sized solutes. We do not expect that such inter-channel effects are pronounced and rather focus on the trans-channel effect.

We can make a rough estimate of the exclusion effect when we assume that the trans-channel term $h_{D,1}$ in Giddings' model is reduced to the same extent as the convective dispersion in an open tube of comparable cross-sectional size after DiMarzio and Guttman [2]. In order to calculate r_p/r_c we then need to assign an equivalent capillary radius to the flow channels in a packed column. As an equivalent radius we obviously choose the hydraulic radius, because it has been shown to be convenient in modelling size effects on retention behaviour in HDC [1,37]. For the column used, we obtain a hydraulic radius of 0.32 μm [28]. Consequently, the r_p/r_c ratios for the polymers used are 0.0034 for PS 2200, 0.020 for PS 43 900 and 0.11 for PS 775 000 [28]. The estimated reduction in ω_1 is then 2%, 11% and 47%, respectively. This reduction seems pronounced but, as it only affects one coupling term, the effect on the overall plate height curve is small. A change in $h_{D,1}$ most severely affects h_{kin} at the higher reduced velocities (see also Fig. 1). At $\nu = 160$ the calculated plate height reduction due to wall exclusion is 0.005 for PS 2200, 0.03 for PS 43 900 and 0.2 for PS 775 000. Under the actual experimental conditions, the shift for PS 2200 and PS 43 900 is even smaller because the reduced velocities for these solutes are smaller.

Hydrodynamic wall effects. When the transport of finite sized particles in small flow channels is considered, hydrodynamic particle-wall interactions should also be accounted for. The role of such interactions in the transport of homogeneous spherical particles in cylindrical tubes has been treated extensively by Brenner and Gaydos [3]. Owing to hydrodynamic wall

effects, the particle diffusivity is not a constant as in unbounded fluids. Rather, axial and transverse diffusivities are functions of the transverse position of the particle, both becoming zero for a sphere in contact with the wall. Consequently, the mean axial molecular diffusion coefficient is diminished below its value in an unbounded fluid. The diffusivity is reduced to a larger extent when the ratio of the particle diameter to the flow channel diameter increases. If we again consider the r_p/r_c values for our packed column, the diffusivity reduction, calculated according to Brenner and Gaydos [3], would be 2%, 7% and 30% for PS 2200, 43 900 and 775 000, respectively. Although these values are strictly valid only for open tubes, they show that a pronounced reduction of diffusivity is also to be expected in our packed column.

Another result of hydrodynamic particle-wall interactions is that the centre of a solute molecule lags the local flow in which it is suspended [1–4]. This hydrodynamic retardation effect (so-called slip flow) also varies with the transverse position of the solute.

When hydrodynamic wall effects are considered together with wall exclusion, the convective dispersion of finite sized particles in an open tube differs from that of zero-sized solutes by a factor of $1 - (1.862r_p/r_c) + 9.68(r_p/r_c)^2$ [3]. From this factor it appears that the finite solute size reduces dispersion compared with infinitely small solutes, provided that the r_p/r_c ratio does not exceed 0.14. If we again depict the interstitial flow channels in a packed column as open tubes, we calculate a reduction in convective dispersion of 0.6%, 3% and 9% for PS 2200, 43900 and 775 000, respectively. These percentages are substantially lower than those given under *Exclusions regions,* where only wall exclusion was considered. Including hydrodynamic wall effects therefore appears to diminish the overall effect of finite solute size on convective dispersion in an open tube. When the impact of both hydrodynamic wall effects and wall exclusion on h_{kin} is calculated (as under *Exclusion regions),* it appears to be negligibly small for the polymer fractions used. If our calculations are in any way able to give realistic estimates of hydrodynamic wall effects and wall exclusion in packed columns, then the overall effect of finite solute

size on dispersion in **packed-column** HDC is negligibly small. This is speculative, however, because applying capillary models to describe **hydrodynamic** wall effects and wall exclusion in packed columns may well prove to be an over-simplification.

Other considerations

In addition to the polydispersity and size effects mentioned above, other factors might also influence the dispersion in packed columns. One important factor might be the distribution of solutes over the accessible radial positions. Until now we assumed this distribution to be uniform, but this need not be so in practice. Owing to, for example, hydrodynamic forces, depletion of macromolecules in the wall regions and enrichment in the centre of a flow channel may occur. Phenomena leading to opposite effects have also been described [28]. A disturbance of the equilibrium concentration **profile** in a flow channel may either increase or decrease dispersion. A pronounced decrease in dispersion has, for example, been reported in open tubes where particles were focused into an annular ring owing to the "tubular pinch" effect [4,38,39]. Possibly a build-up of a transverse concentration profile occurs also in flow channels in a packed column. However, the effect on h is expected to be smaller than in open tubes, for the **following** reasons. First, a build-up of a concentration profile in packed columns is counteracted by stream splitting and other **randomizing** flow phenomena. Second, a concentration profile mainly has a short-range effect, just like wall exclusion. In terms of **Giddings'** plate height model, a concentration profile will influence the trans-channel effect, but will not change dispersion resulting from velocity differences existing between neighbouring channels or between certain regions in the column. By changing only one coupling term, the effect of a non-uniform concentration profile on the measured plate height will be relatively small. Accurate estimates are unfortunately obstructed by the complex flow pattern in packed columns.

CONCLUSIONS

In packed-column HDC, the reduced plate

heights for polystyrenes of widely differing molecular masses and toluene appear to lie on one smooth line. Measured reduces plate heights, in a wide range of reduced velocities, are in good accordance with both Giddings' theoretical model and the Knox semi-empirical model for the dispersion of small molecules in packed infinite diameter columns. The measured plate heights indicate that the effect of the disturbed packing near the column wall and other trans-column effects do not influence zone broadening to a large extent. For the higher molecular masses (which are of actual interest in HDC), the main kinetic source of zone spreading is the random flow in a packed column. The polydispersity of the solutes appears to be a severe limitation for obtaining h_{kin} in the high selectivity region of the HDC calibration graph. The effect of size and hydrodynamic particle-wall interactions on dispersion in packed column HDC cannot be determined exactly. According to approximate theoretical calculations and available experimental evidence, they do not affect h to a large extent.

ACKNOWLEDGEMENTS

REFERENCES

1 A.J. McHugh, CRC *Crit. Rev. Anal. Chem.,* 15 (1984) 63.
2 E.A. DiMarzio and C.M. Guttman, *Macromolecules, 3 (1970) 131* and 681.
3 H. Brenner and L.J. Gaydos, *J. Colloid Interface Sci., 58 (1977) 312.*
4 H.J. Ploehn, *Znt. J. Multiphase Flow, 13 (1987) 773.*
5 R. Tijssen, J. Bos and M.E. van Kreveld, *Anal. Chem., 58 (1986) 3036.*
6 H. Small, *J. Colloid Interface Sci., 48 (1974) 147.*
7 R.F. Stoisits, G.W. Poehlein and J.W. Vanderhoff, *J. Colloid Interface Sci., 64 (1978) 201.*
8 P.G. Saffman, *J. Fluid Mech., 7* (1960) 194.
9 C.A. Silebi and J.P. Viola, Org. *Coat. Plast. Chem.,* 42 (1980) 151.
10 H. Brenner, *Philos. Trans. R. Soc. London, Ser. A, 297 (1980)* 81.
11 H. Brenner and P.M. Adler, *Philos. Trans. R. Soc. London, Ser. A, 307 (1982) 149.*
12 J.C. Giddings, *J. Chromatogr., 5 (1961) 61.*
13 C. Horváth and H.J. Lin, *J. Chromatogr., 126 (1976) 401.*
14 J.F.K. Huber, *J. Chromatogr. Sci., 7 (1969) 85.*
15 J.N. Done and J.H. Knox, *J. Chromatogr. Sci.,* 10 (1972) 606.
16 J.C. Giddings, *Dynamics of Chromatography. Pan 1. Principles and Theory,* Marcel Dekker, New York, 1965.
17 J.C. Giddings, *Unified Separation Science,* Wiley-Interscience, New York, 1991.
18 J.H. Knox and L. McLaren, *Anal.* Chem., 36 (1964) 1477.
19 J.H. Knox, *Anal. Chem., 38 (1966) 253.*
20 J.H. Knox and J.F. Parcher, *Anal.* Chem., 41 (1969) 1599.
21 J.H. Knox, *J. Chromatogr. Sci., 15 (1977) 352.*
22 G.J. Kennedy and J.H. Knox, *J. Chromatogr. Sci.,* 10 (1972) 549.
23 R.W. Stout, J.J. DeStefano and L.R. Snijder, *J. Chromatogr., 282 (1983) 263.*
24 J.N. Done, J.H. Knox and J. Loheac, *Applications of High-Speed Liquid Chromatography,* Wiley-Interscience, London, 1974, Ch. 4.
25 R.T. Kennedy and J.W. Jorgenson, *Anal. Chem., 61 (1989) 1128.*
26 K.E. Karlsson and M. Novotny, *Anal.* Chem., 60 (1988) 1662.
27 J.H. Knox, G.R. Laird and P.A. Raven, *J. Chromatogr., 122 (1976) 129.*
28 J.C. Kraak, H. Poppe and R. Tijssen, in preparation.
29 R.C. Reid, J.M. Prausnitz and T.K. Sherwood, *The Properties of Gases and Liquids,* McGraw-Hill, New York, 3rd ed., 1977.
30 W. Mandema and H. Zeldenrust, *Polymer,* 18 (1977) 835.
31 J.H. Knox and F. McLennan, *Chromatographia,* 10 (1977) 75.
32 G. Stegeman, J.C. Kraak and H. Poppe, *J. Chromatogr., 550 (1991) 721.*
33 M.E. Schimpf, P.S. Williams and J.C. Giddings, *J. Appl. Polym. Sci., 37 (1989) 2059.*
34 M.E. Schimpf, M.N. Meyers and J.C. Giddings, *J. Appl. Polym. Sci., 33 (1987) 117.*
35 F.P. Warner, personal communication.
36 J.C. Giddings, *Sep. Sci. Technol., 13 (1978) 241.*
37 G. Stegeman, R. Oostervink, J.C. Kraak, H. Poppe and K.K. Unger, *J. Chromatogr., 506 (1990) 547.*
38 R.J. Noel, K. Gooding, F.E. Regnier, D.M. Ball, C. Orr and H.E. Mullins, *J. Chromatogr.,* 166 (1978) 373.
39 R. Tijssen, in F. Dondi and G. Guiochon (Editors), *Theoretical Advancement in Chromatography and Related Separation Techniques,* Kluwer, Dordrecht, 1992, pp. 397-441.